Supplementary Material: Complementary screening for quantum spin Hall insulators in two-dimensional exfoliable materials

Davide Grassano,[1, *] Davide Campi,[1, 2] Antimo Marrazzo,[1, 3] and Nicola Marzari[1]

[1] *Theory and Simulations of Materials (THEOS) and National Center for Computational Design and Discovery of Novel Materials (MARVEL), École Polytechnique Fédérale de Lausanne, CH-1015 Lausanne, Switzerland*

[2] *Dipartimento di Scienza dei Materiali, Universita di Milano-Bicocca, Via Cozzi 53, 20125 Milano, Italy*

[3] *Dipartimento di Fisica, Università di Trieste, I-34151 Trieste, Italy*

Quantum spin Hall insulators are a class of topological materials that has been extensively studied during the past decade. One of their distinctive features is the presence of a finite band gap in the bulk and gapless, topologically protected edge states that are spin-momentum locked. These materials are characterized by a $\mathbb{Z}_2$ topological order where, in the 2D case, a single topological invariant can be even or odd for a trivial or a topological material, respectively. Thanks to their interesting properties, such as the realization of dissipationless spin currents, spin pumping and spin filtering, they are of great interest in the field of electronics, spintronics and quantum computing. In this paper we perform an high-throughput screening of quantum spin Hall insulators starting from a set of 783 two-dimensional exfoliable materials, recently identified from a systematic screening of the ICSD, COD, and MPDS databases. We find a new $\mathbb{Z}_2$ topological insulator ($Hg_4N_4S_4$) as well as 3 already known ones and 7 direct gap metals that have the potential of becoming quantum spin Hall insulators under a reasonable external perturbation.

I. CONTENT SUMMARY

Here we present a summary of the data for every material determined to be either a quantum spin Hall insulator or a direct gap metal. For the entire collection of materials we show a statistical analysis of the space groups and cell volumes, in relation to the topology. For each, we report a table of the structural parameters, including the direct lattice vectors and the positions of the atoms in the relaxed structure. We also show the band structure, both with and without SOC, and, for non inversion-symmetric materials we also show the plot of the HWCC evolution. Finally, for every material we also show a bird-eye view of its crystal structure rendered using VESTA[1].

II. STATISTICAL ANALYSIS

Here we report a statistical analysis of the starting datasets for this work and the preceding one from Marrazzo et al[2]. In Fig. SM1 and SM3 we show the distribution of the original dataset in term of Bravais lattices and spacegroups. From this analysis we can observe that the spacegroup 11 from the monoclinic Bravais lattice seems to bring a significant contribution to the abundance of $\nu = 1$ materials. Conversely, spacegroups from the tetragonal Bravais lattice seems to be relatively void of $\nu = 1$ materials. In Fig. SM2 and SM4 we show a distribution of the material in term of cell volume for the present and preceding dataset respectively. From the analysis of both datasets a clear correlation between cell volume and topology cannot be drawn. While the plots might suggest that $\nu = 1$ materials are concentrated in the region of lower cell volumes, it should also be considered that materials with greater cell sizes/number of atoms are excluded from these screening due to the high computational costs involved that would not be feasible in an high-throughput study.
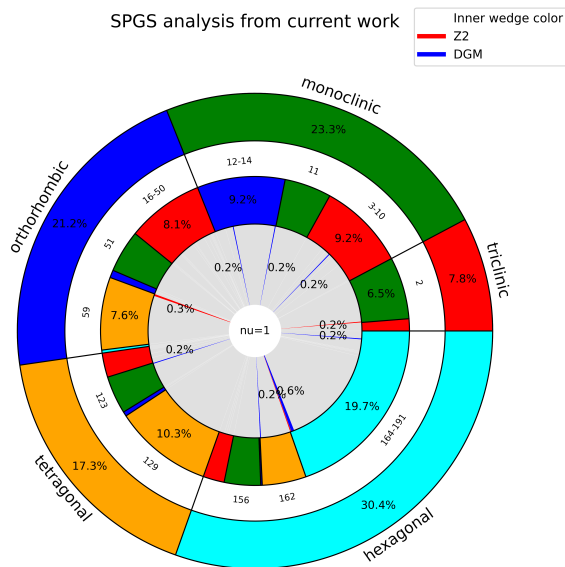
FIG. SM1: Bravais lattice and spacegroup analysis of the dataset analysed in this work. Space groups with occurrence lower than 3% have been grouped together. In the inner section of the pie chart, the red(blue) slices indicates the QSHIs(DGMs) originating from the corresponding space group in the central section of the chart
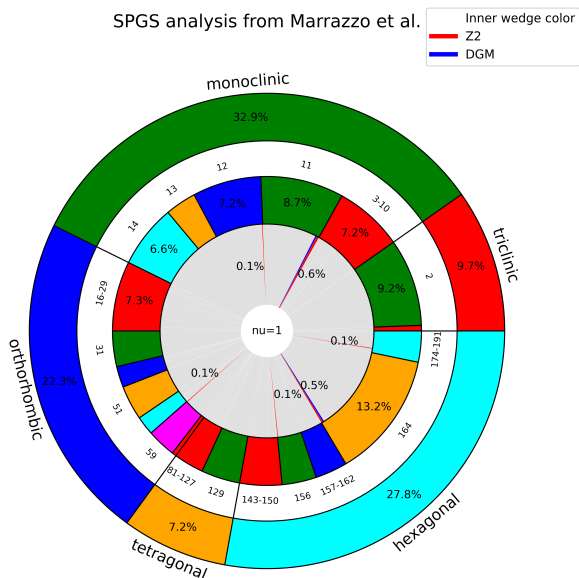

FIG. SM3: Bravais lattice and spacegroup analysis of the dataset analysed in the previous work from Marrazzo et al. Space groups with occurrence lower than 3% have been grouped together. In the inner section of the pie chart, the red(blue) slices indicates the QSHIs(DGMs) originating from the corresponding space group in the central section of the chart
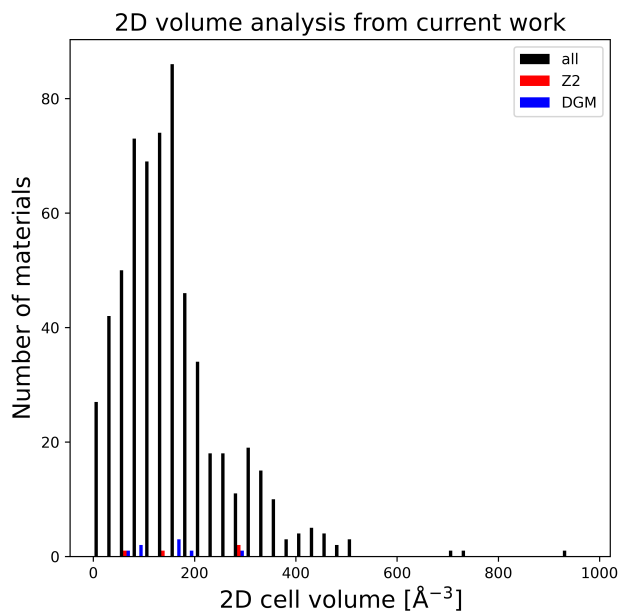

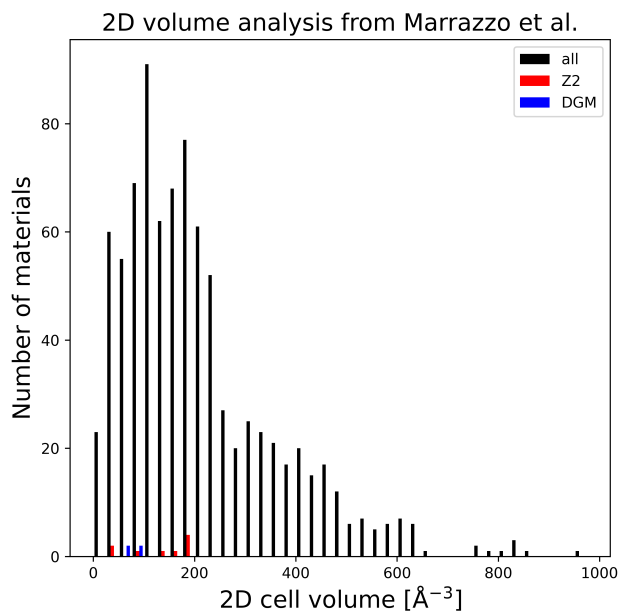FIG. SM2: Cell volume analysis of the dataset analysed in this work.

FIG. SM4: Cell volume analysis of the dataset analysed in the previous work from Marrazzo et al.

III. QSHI

A. HfBr

Unit formula	:	Br_2Hf_2
Database ID	:	MPDS S546529
3D Spacegroup	:	166 ($R\bar{3}m$)
Inversion symmetry	:	YES
Direct Gap [meV]	:	232.8
Indirect gap [meV]	:	48.3
Binding energy DF2-C09 [meV/Å^2]	:	15.8

TABLE SM1: Structural parameters

	X[Å]	Y[Å]	Z[Å]
a1	1.7402	-3.0141	0.0000
a2	1.7402	3.0141	0.0000
a3	0.0000	0.0000	24.0847
Hf	1.7402	1.0047	-1.1321
Br	0.0000	0.0000	-3.0392
Hf	1.7402	-1.0047	1.1321
Br	0.0000	0.0000	3.0392
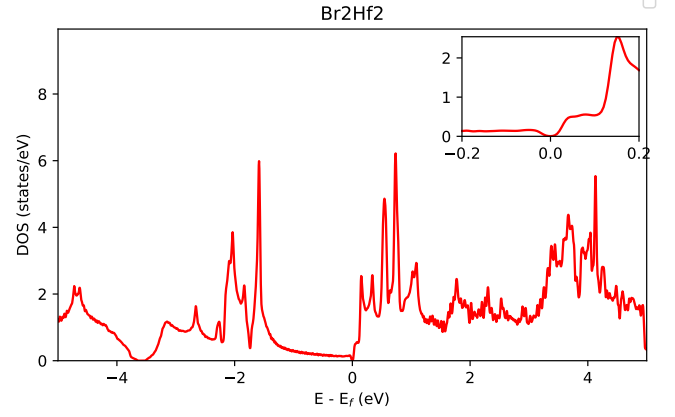
FIG. SM6: DFT density of states. The insets shows the range around the Fermi level.

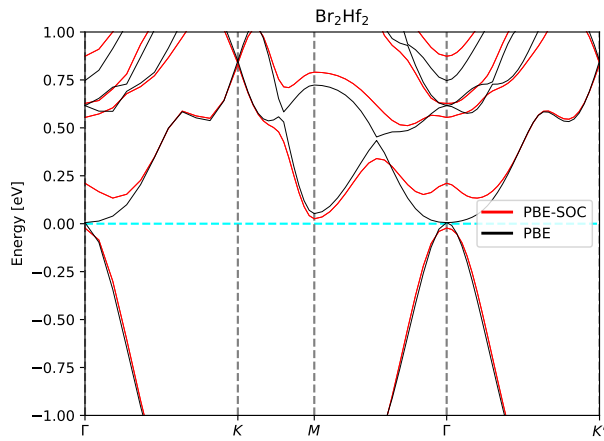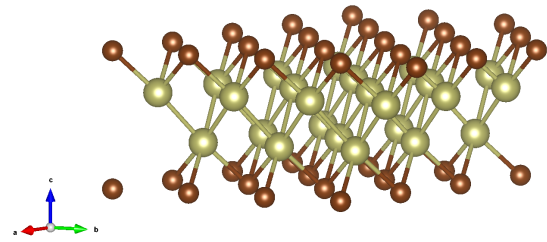FIG. SM5: DFT band structure with (red) and without (black) spin-orbit coupling.

FIG. SM7: Bird-eye view of the crystal structure.

B.   HfTe$_5$

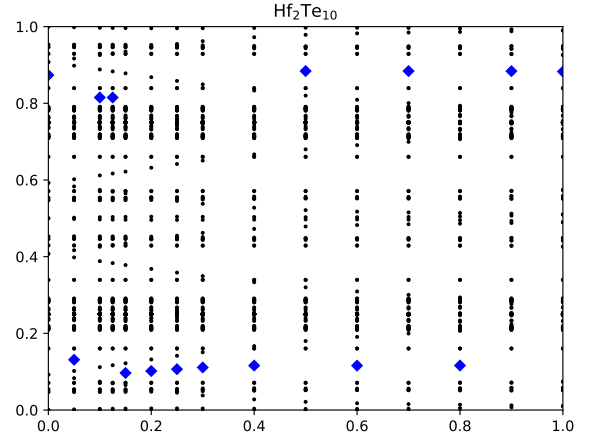|	
Unit formula:	Hf$_2$Te$_{10}$
Database ID:	MPDS S455329
3D Spacegroup:	63 (Cmcm)
Inversion symmetry:	NO
Direct Gap [meV]:	299.3
Indirect gap [meV]:	171.0
Binding energy DF2-C09 [meV/Å^2]:	16.5

FIG. SM10: Evolution of the HWCC (black dots) and largest gap positions (blue squares) across the Brillouin zone.
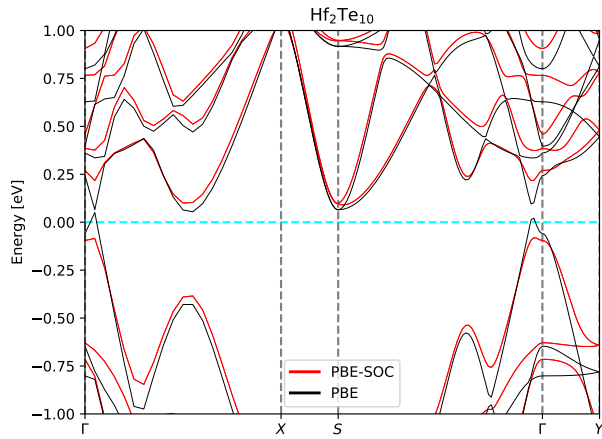

FIG. SM8: DFT band structure with (red) and without (black) spin-orbit coupling.
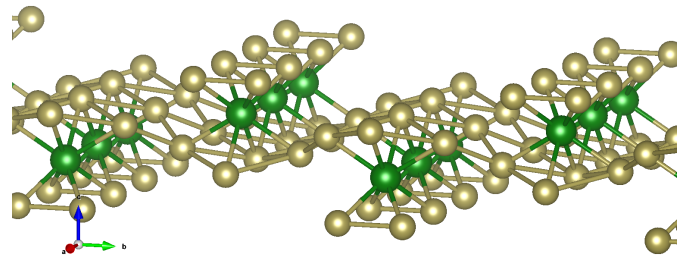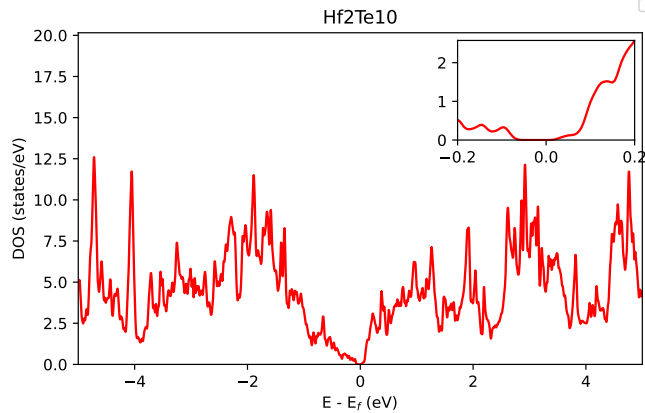

FIG. SM11: Bird-eye view of the crystal structure.

FIG. SM9: DFT density of states. The insets shows the range around the Fermi level.

TABLE SM2: Structural parameters

	X[Å]	Y[Å]	Z[Å]
a1	4.0291	0.0000	0.0000
a2	0.0000	13.8324	0.0000
a3	0.0000	0.0000	22.3851
Hf	-1.0073	-17.2905	-0.9906
Hf	1.0073	-10.3743	0.9906
Te	1.0073	-17.2905	1.2315
Te	-1.0073	-10.3743	-1.2315
Te	-1.0073	-19.8333	0.5747
Te	1.0073	-12.9171	-0.5747
Te	1.0073	-7.8316	-0.5747
Te	-1.0073	-14.7478	0.5747
Te	1.0073	-15.8953	-2.6504
Te	-1.0073	-8.9790	2.6504
Te	-1.0073	-11.7696	2.6504
Te	1.0073	-18.6858	-2.6504

C.   HgNS

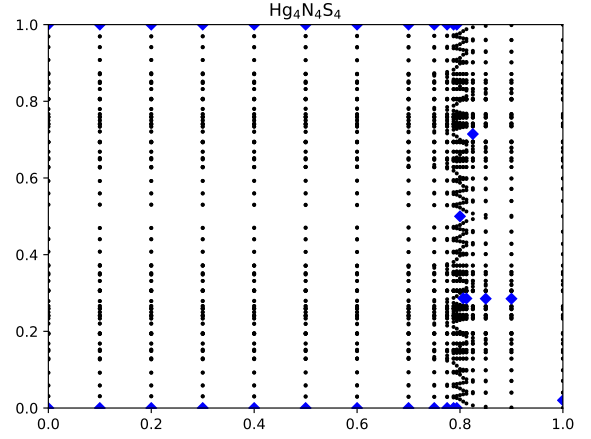|	
Unit formula:	$Hg_4N_4S_4$
Database ID:	MPDS S1703098
3D Spacegroup:	61 (Pbca)
Inversion symmetry:	NO
Direct Gap [meV]:	7.1
Indirect gap [meV]:	7.1
Binding energy DF2-C09 [meV/Å^2]:	19.4

FIG. SM14: Evolution of the HWCC (black dots) and largest gap positions (blue squares) across the Brillouin zone.
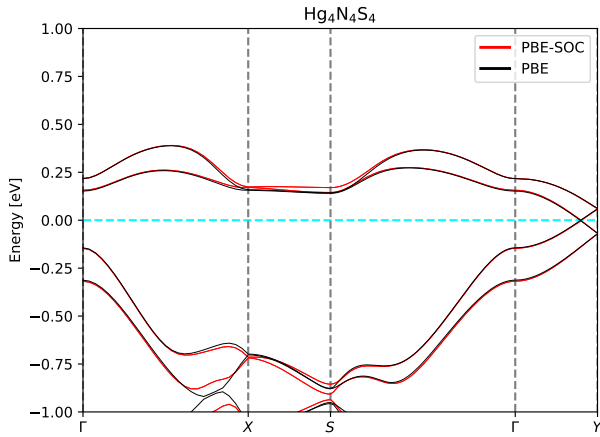

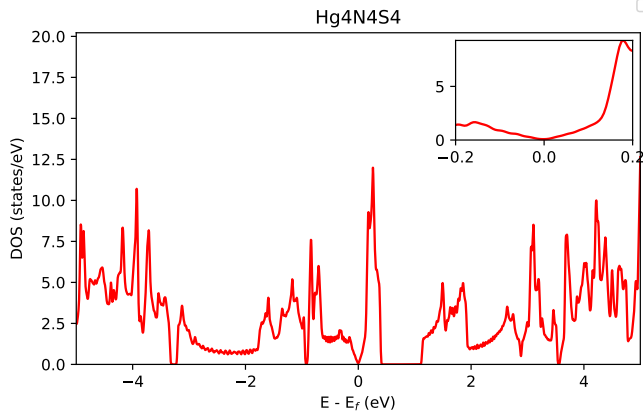FIG. SM12: DFT band structure with (red) and without (black) spin-orbit coupling.

FIG. SM15: Bird-eye view of the crystal structure.

TABLE SM3: Structural parameters

	X[Å]	Y[Å]	Z[Å]
a1	5.3686	-0.0018	0.0000
a2	-0.0201	10.7795	0.0000
a3	0.0000	0.0000	16.9180
Hg	-6.4161	1.4264	0.5240
Hg	-3.7342	3.9802	-0.5538
Hg	-4.3412	9.3567	-0.5240
Hg	-7.0231	6.8029	0.5538
S	-6.6170	-0.8389	-1.2004
S	-3.9513	6.2104	1.2206
S	-4.1202	0.8425	1.2004
S	-6.8060	4.5727	-1.2206
N	-7.6635	8.8272	-0.6895
N	-4.9765	7.3325	0.7252
N	-3.0938	1.9559	0.6895
N	-5.7808	3.4506	-0.7252

FIG. SM13: DFT density of states. The insets shows the range around the Fermi level.
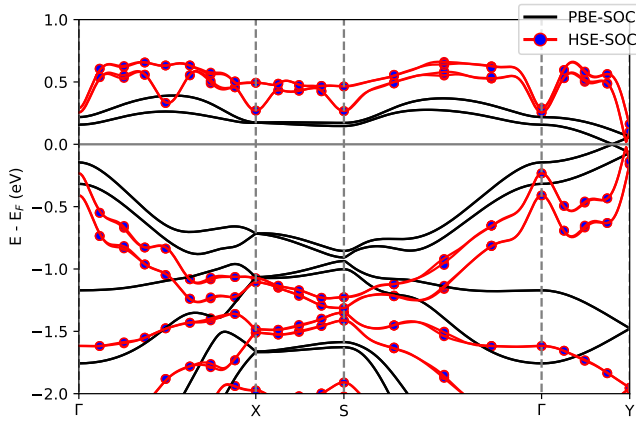
FIG. SM16: DFT-PBE and HSE06 band structures for HgNS. It can be observed that the gap widens in the HSE calculation, moving the quasi-linear crossing toward the edge of the zone; still, this is not strong enough to remove the band inversion.
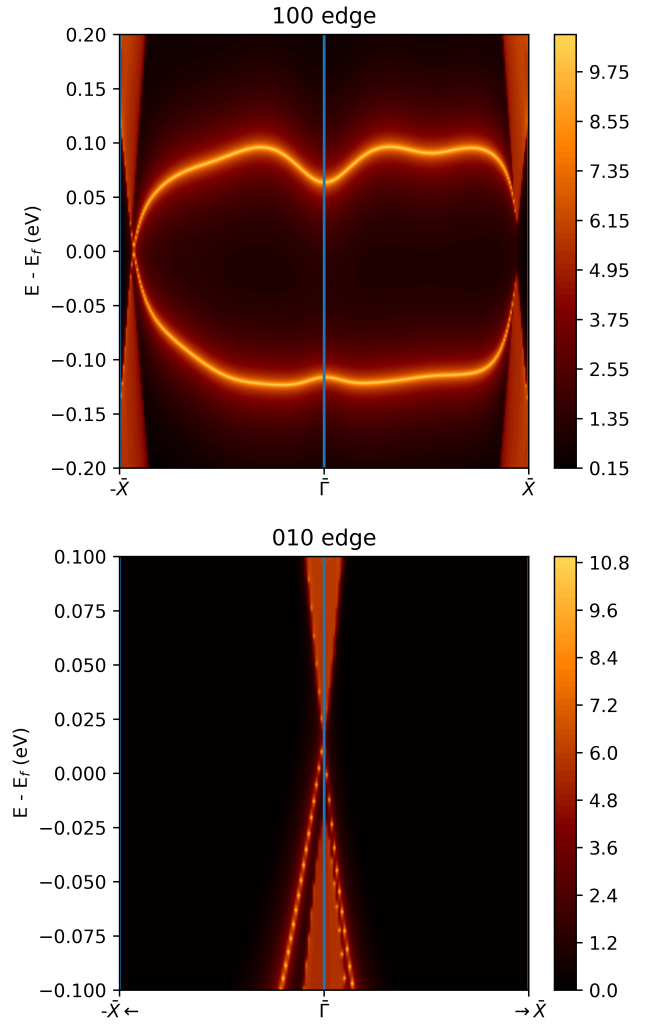

FIG. SM18: Edge states of HgNS computed using WannierTools starting from the Wannier Hamiltonian computed at the HSE level, with respect to the 100 and 010 edges (top and bottom panel respectively). The bulk quasi-linear crossing can be observed for the 100 (010) edge in proximity of the $\bar{X}$ ($\bar{\Gamma}$) high-symmetry point. Edge states leaking from the bulk states are also visible: they connects the valence and conduction bulk bands while crossing the gap, which is the hallmark of a topological edge state.
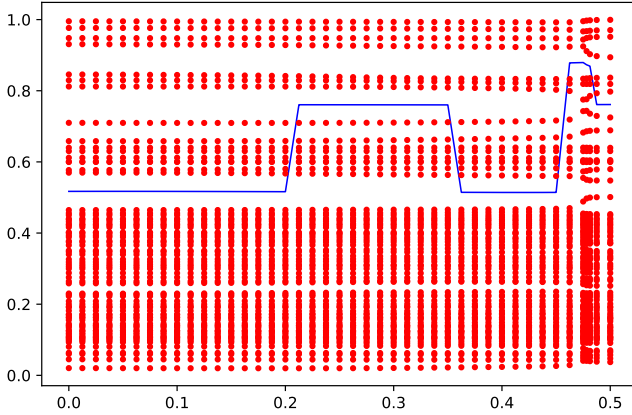

FIG. SM17: Evolution of the HWCCs computed using WannierTools starting from the Wannier Hamiltonian computed at the HSE level.

D. ZrTe₅

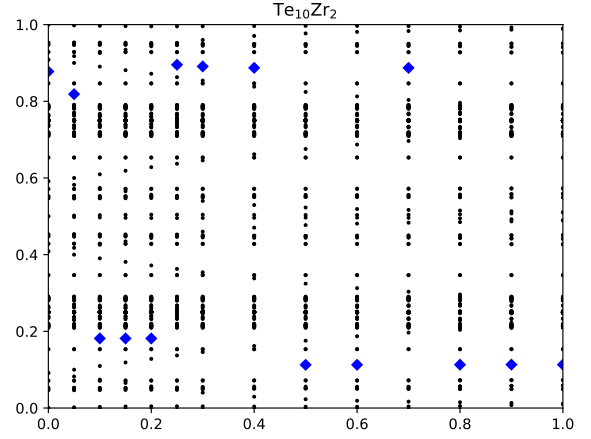|	
Unit formula:	$Te_{10}Zr_2$
Database ID:	MPDS S457010
3D Spacegroup:	63 (Cmcm)
Inversion symmetry:	NO
Direct Gap [meV]:	280.7
Indirect gap [meV]:	219.6
Binding energy DF2-C09 [meV/Å²]:	19.4

FIG. SM21: Evolution of the HWCC (black dots) and largest gap positions (blue squares) across the Brillouin zone.
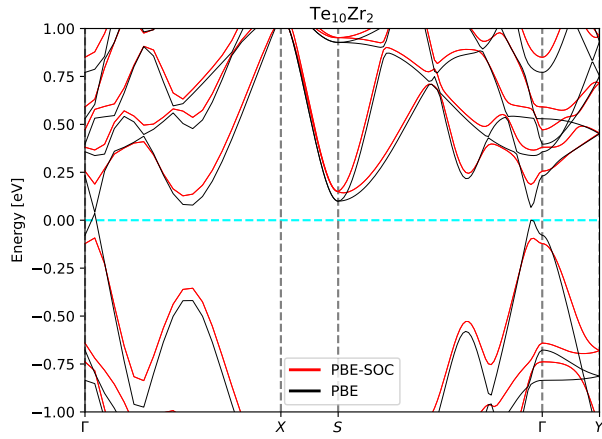

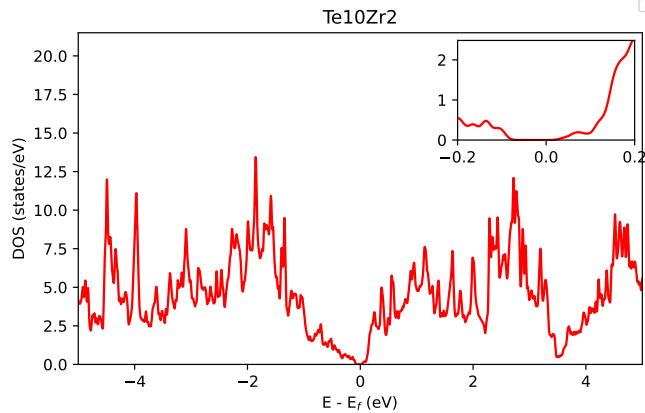FIG. SM19: DFT band structure with (red) and without (black) spin-orbit coupling.

FIG. SM22: Bird-eye view of the crystal structure.

FIG. SM20: DFT density of states. The insets shows the range around the Fermi level.

TABLE SM4: Structural parameters

	X[Å]	Y[Å]	Z[Å]
a1	4.0472	0.0000	0.0000
a2	0.0000	13.8438	0.0000
a3	0.0000	0.0000	22.4715
Zr	1.0118	-10.3829	-1.0016
Zr	-1.0118	-3.4610	1.0016
Te	-1.0118	-11.7748	-2.6768
Te	1.0118	-2.0690	2.6768
Te	-1.0118	-8.9910	-2.6768
Te	1.0118	-4.8529	2.6768
Te	-1.0118	-10.3829	1.2327
Te	1.0118	-3.4610	-1.2327
Te	1.0118	-7.8333	0.5745
Te	-1.0118	-6.0105	-0.5745
Te	1.0118	-12.9324	0.5745
Te	-1.0118	-0.9114	-0.5745

IV.   DGM

A.   BaCr$_2$N$_2$O$_8$

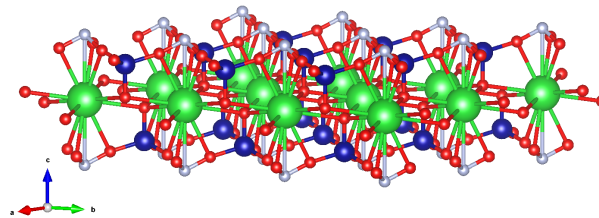|	
Unit formula:	BaCr$_2$N$_2$O$_8$
Database ID:	MPDS S1704934
3D Spacegroup:	166 (R$\bar{3}$m)
Inversion symmetry:	YES
Direct Gap [meV]:	19.3
Indirect gap [meV]:	-124.0
Binding energy DF2-C09 [meV/Å^2]:	11.0

FIG. SM25: Bird-eye view of the crystal structure.
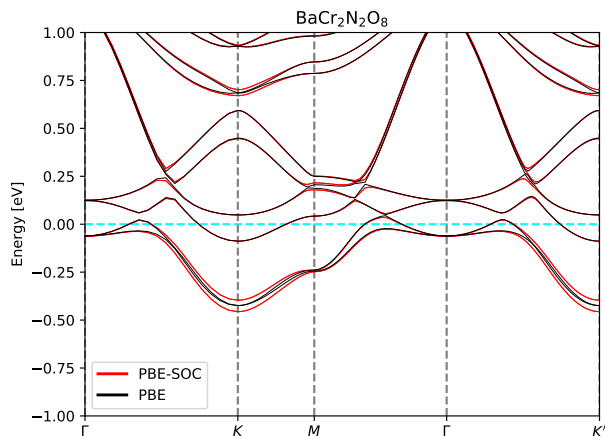
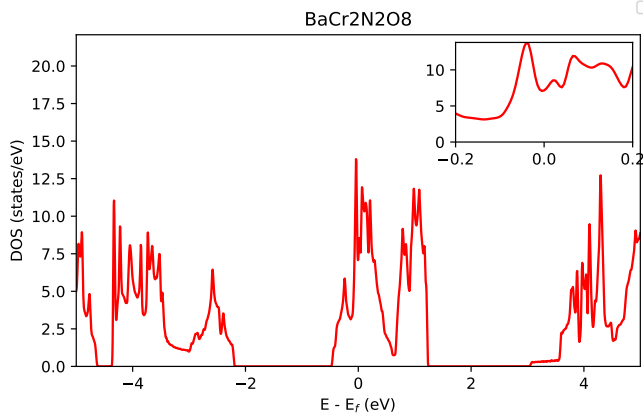FIG. SM23: DFT band structure with (red) and without (black) spin-orbit coupling.

TABLE SM5: Structural parameters

	X[Å]	Y[Å]	Z[Å]
a1	2.6064	-4.5145	0.0000
a2	2.6064	4.5145	0.0000
a3	0.0000	0.0000	24.7486
Cr	3.9097	-0.7524	2.1565
N	1.3032	-2.2572	3.2679
O	2.4168	-1.6143	2.6330
O	1.3032	-3.5431	2.6330
O	0.1897	-1.6143	2.6330
O	1.3032	0.7524	-0.4977
Cr	1.3032	0.7524	-2.1565
N	1.3032	-2.2572	-3.2679
O	2.4168	-2.9002	-2.6330
O	1.3032	-0.9714	-2.6330
O	0.1897	-2.9002	-2.6330
O	3.9097	-0.7524	0.4977
Ba	1.3032	-2.2572	0.0000

FIG. SM24: DFT density of states. The insets shows the range around the Fermi level.

B.   VBr$_3$

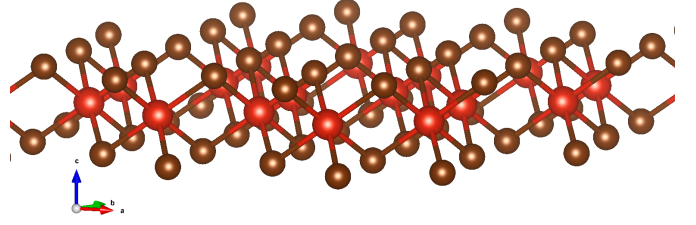|	
Unit formula:	Br$_6$V$_2$
Database ID:	MPDS S1902638
3D Spacegroup:	148 (R$\bar{3}$)
Inversion symmetry:	YES
Direct Gap [meV]:	32.9
Indirect gap [meV]:	-99.4
Binding energy DF2-C09 [meV/Å^2]:	15.1

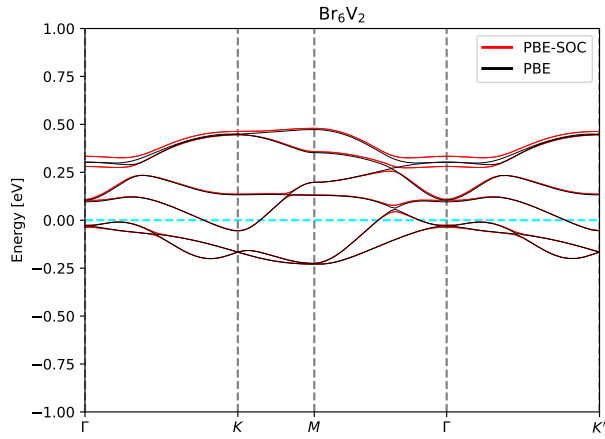FIG. SM28: Bird-eye view of the crystal structure.

FIG. SM26: DFT band structure with (red) and without (black) spin-orbit coupling.

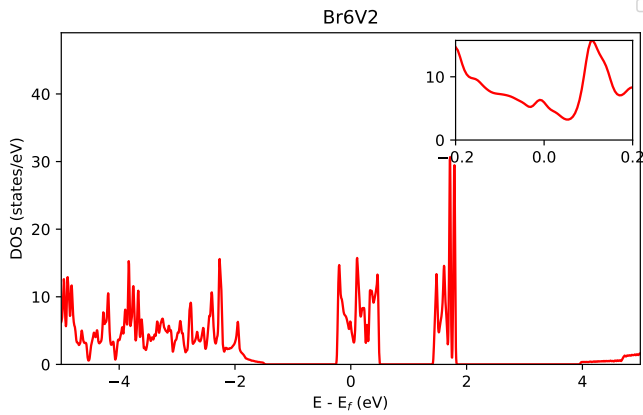

FIG. SM27: DFT density of states. The insets shows the range around the Fermi level.

TABLE SM6: Structural parameters

	X[Å]	Y[Å]	Z[Å]
a1	3.1108	5.3881	0.0000
a2	-3.1108	5.3881	0.0000
a3	0.0000	0.0000	17.9200
V	0.0000	-3.5920	0.0000
V	-3.1108	-1.7960	0.0000
Br	-4.1801	-3.5359	-1.4813
Br	-2.1386	0.0000	1.4813
Br	-2.0415	-3.5359	1.4813
Br	-5.1523	-1.8521	1.4813
Br	-4.0830	0.0000	-1.4813
Br	-1.0693	-1.8521	-1.4813

C.   FePO$_4$(CH$_3$)

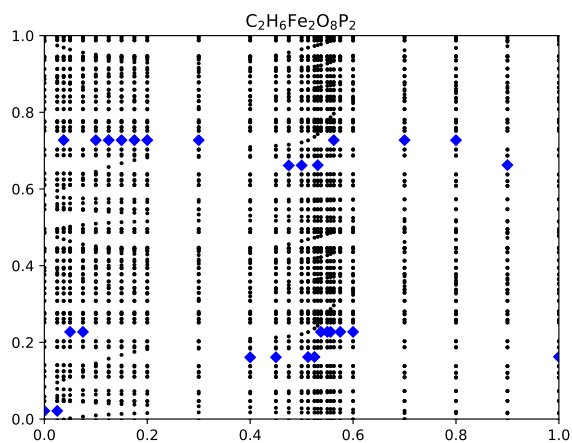|	
Unit formula:	C$_2$H$_6$Fe$_2$O$_8$P$_2$
Database ID:	MPDS S1125577
3D Spacegroup:	2 (P$\bar{1}$)
Inversion symmetry:	NO
Direct Gap [meV]:	10.7
Indirect gap [meV]:	-58.4
Binding energy DF2-C09 [meV/Å^2]:	18.8

FIG. SM31: Evolution of the HWCC (black dots) and largest gap positions (blue squares) across the Brillouin zone.
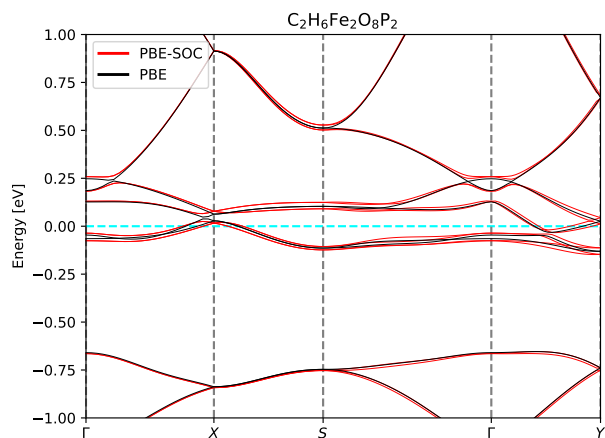

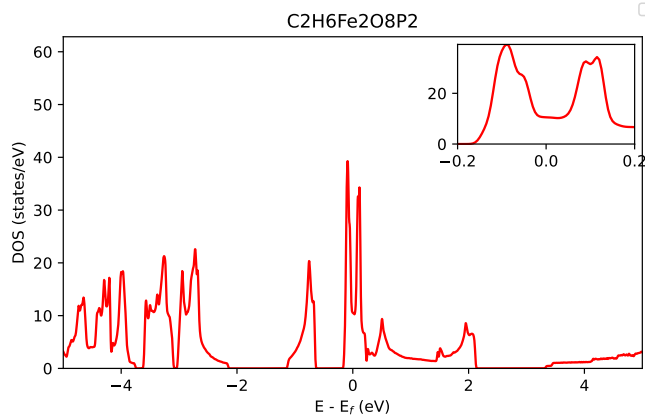FIG. SM29: DFT band structure with (red) and without (black) spin-orbit coupling.

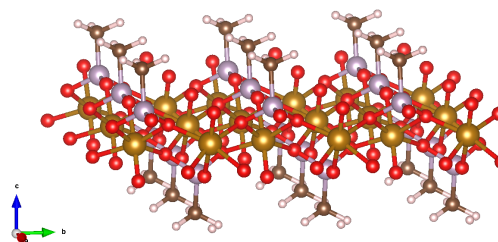FIG. SM30: DFT density of states. The insets shows the range around the Fermi level.

FIG. SM32: Bird-eye view of the crystal structure.

TABLE SM7: Structural parameters

	X[Å]	Y[Å]	Z[Å]
a1	4.7069	0.0001	0.0000
a2	0.0001	5.5134	0.0000
a3	0.0000	0.0000	27.1570
Fe	1.7832	1.0894	-0.1656
Fe	4.1367	3.8461	0.1656
P	1.4160	3.8460	-1.5644
P	3.7694	1.0894	1.5644
H	1.3837	4.7506	-3.7631
H	3.7371	1.9939	3.7631
H	4.5854	3.8392	-3.3781
H	2.2320	1.0825	3.3781
H	1.3963	2.9503	-3.7671
H	3.7497	0.1936	3.7671
C	0.9711	3.8464	-3.2992
C	3.3245	1.0898	3.2992
O	0.6460	2.6491	-0.8231
O	2.9995	5.4058	0.8231
O	0.6459	5.0429	-0.8229
O	2.9993	2.2862	0.8229
O	2.9250	3.8461	-1.4274
O	0.5715	1.0894	1.4274
O	2.5717	1.0893	-1.6026
O	0.2183	3.8460	1.6026

D. HfCl

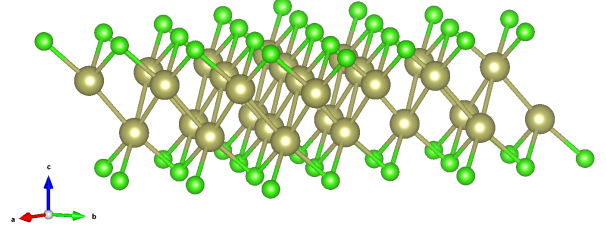|	
Unit formula:	Cl_2Hf_2
Database ID:	MPDS S541493
3D Spacegroup:	166 ($R\bar{3}m$)
Inversion symmetry:	YES
Direct Gap [meV]:	264.5
Indirect gap [meV]:	-165.5
Binding energy DF2-C09 [meV/Å^2]:	14.8

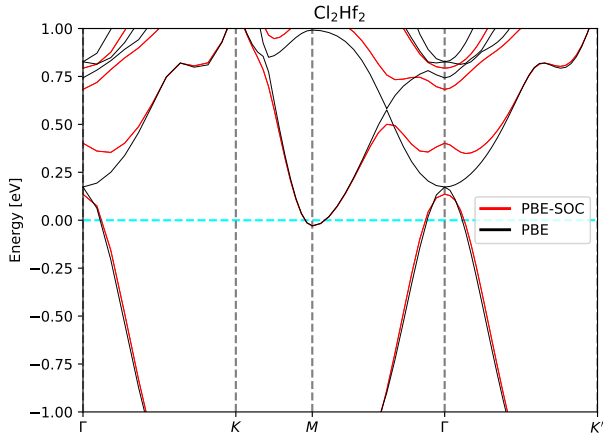FIG. SM35: Bird-eye view of the crystal structure.

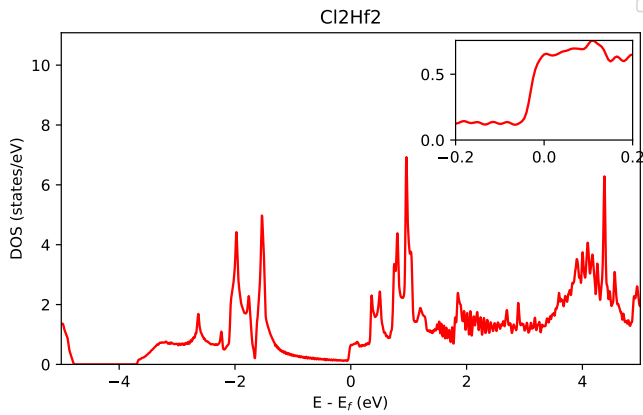FIG. SM33: DFT band structure with (red) and without (black) spin-orbit coupling.

FIG. SM34: DFT density of states. The insets shows the range around the Fermi level.

TABLE SM8: Structural parameters

	X[Å]	Y[Å]	Z[Å]
a1	1.6926	-2.9316	0.0000
a2	1.6926	2.9316	0.0000
a3	0.0000	0.0000	23.5715
Hf	0.0000	0.9772	-1.1509
Cl	1.6926	0.0000	-2.9083
Hf	0.0000	-0.9772	1.1509
Cl	1.6926	0.0000	2.9083

E. Fe₂O₃

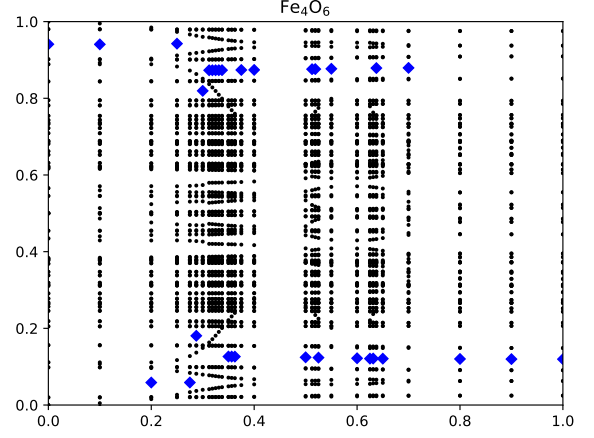|	
Unit formula:	Fe_4O_6
Database ID:	MPDS S1024644
3D Spacegroup:	63 (Cmcm)
Inversion symmetry:	YES
Direct Gap [meV]:	17.4
Indirect gap [meV]:	-20.9
Binding energy DF2-C09 [meV/Å²]:	6.4

FIG. SM38: Evolution of the HWCC (black dots) and largest gap positions (blue squares) across the Brillouin zone.

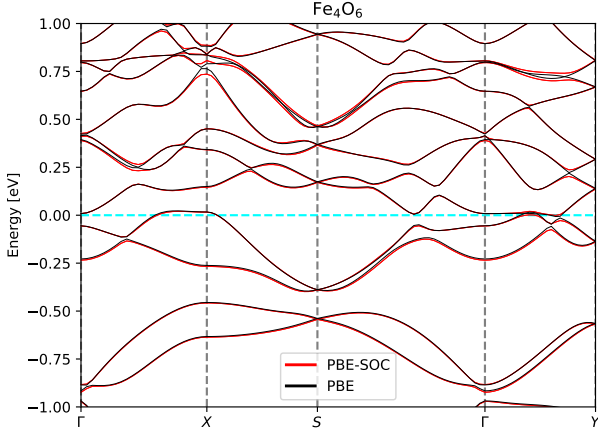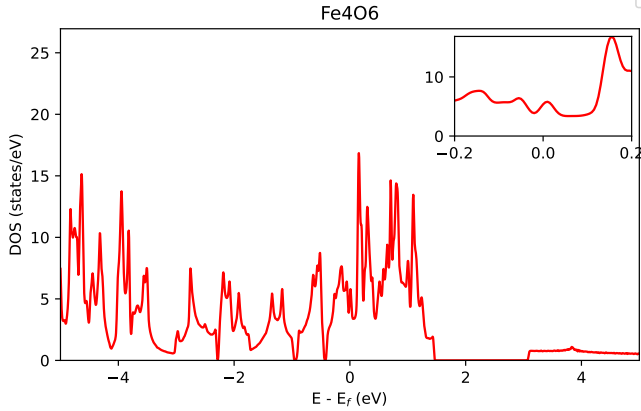FIG. SM36: DFT band structure with (red) and without (black) spin-orbit coupling.

FIG. SM39: Bird-eye view of the crystal structure.

FIG. SM37: DFT density of states. The insets shows the range around the Fermi level.

TABLE SM9: Structural parameters

	X[Å]	Y[Å]	Z[Å]
a1	0.0000	-4.4401	0.0000
a2	5.0537	0.0000	0.0000
a3	0.0000	0.0000	20.2558
Fe	4.7399	-1.2408	0.6055
Fe	2.2130	-3.1992	0.6055
O	4.5735	-1.8252	2.0631
O	2.0466	-2.6149	2.0631
Fe	2.8407	-1.2408	-0.6055
Fe	0.3138	-3.1992	-0.6055
O	3.0071	-1.8252	-2.0631
O	0.4802	-2.6149	-2.0631
O	1.2634	-0.3507	0.0000
O	3.7903	-4.0893	0.0000

F.   MoI$_2$S$_2$

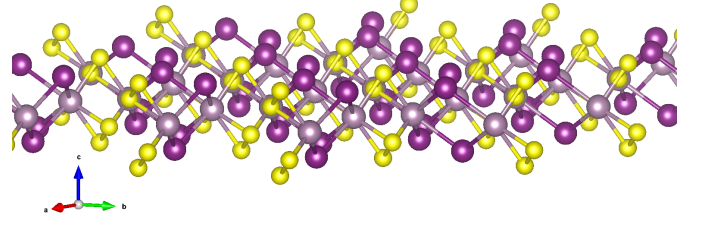|	
Unit formula:	I$_4$Mo$_2$S$_4$
Database ID:	MPDS S376458
3D Spacegroup:	12 (C2/m)
Inversion symmetry:	YES
Direct Gap [meV]:	47.0
Indirect gap [meV]:	-116.5
Binding energy DF2-C09 [meV/Å^2]:	14.4

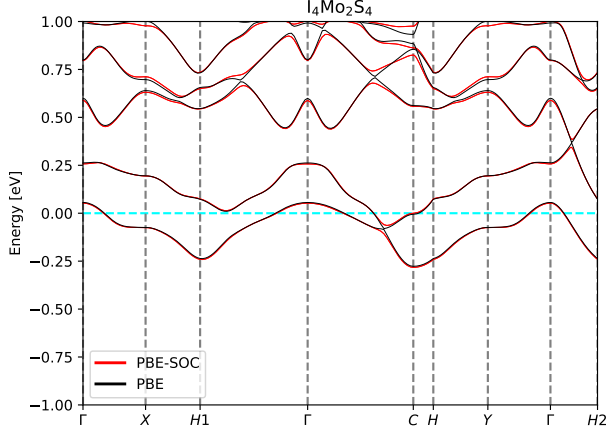FIG. SM42: Bird-eye view of the crystal structure.

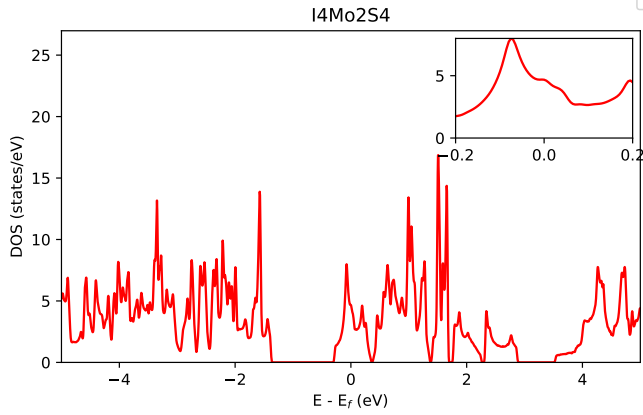FIG. SM40: DFT band structure with (red) and without (black) spin-orbit coupling.

FIG. SM41: DFT density of states. The insets shows the range around the Fermi level.

TABLE SM10: Structural parameters

	X[Å]	Y[Å]	Z[Å]
a1	3.6777	-5.7905	0.0000
a2	3.6777	5.7905	0.0000
a3	0.0000	0.0000	19.9256
I	-1.1916	2.3325	1.5943
I	-1.1916	9.2484	1.5943
Mo	0.0000	4.3943	0.0000
Mo	0.0000	7.1866	0.0000
I	-2.4861	8.1229	-1.5943
I	-2.4861	3.4580	-1.5943
S	-1.7536	5.7905	0.9604
S	0.0294	5.7905	1.9731
S	1.7536	5.7905	-0.9604
S	-0.0294	5.7905	-1.9731

G. $Mo_2Ta_2O_{17}$

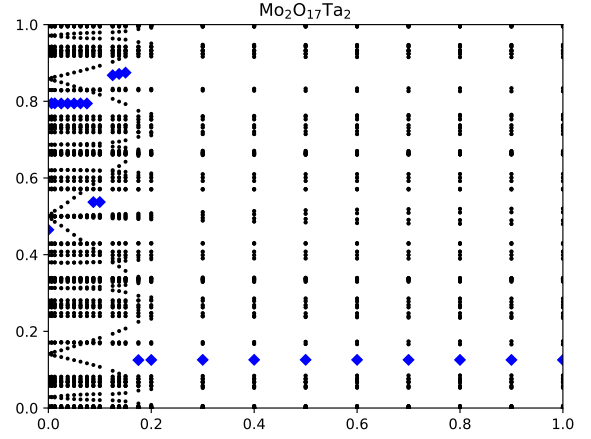|	
Unit formula:	$Mo_2O_{17}Ta_2$
Database ID:	ICSD 247163
3D Spacegroup:	166 ($R\bar{3}m$)
Inversion symmetry:	NO
Direct Gap [meV]:	16.9
Indirect gap [meV]:	-36.3
Binding energy DF2-C09 [meV/Å^2]:	10.0

FIG. SM45: Evolution of the HWCC (black dots) and largest gap positions (blue squares) across the Brillouin zone.
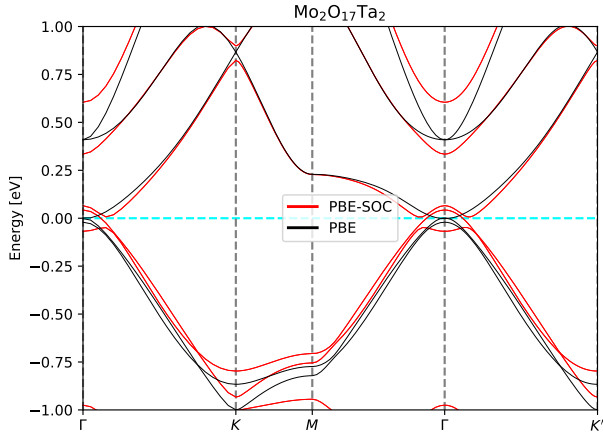

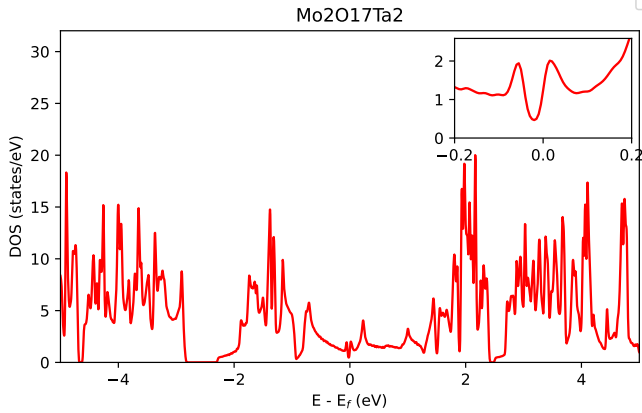FIG. SM43: DFT band structure with (red) and without (black) spin-orbit coupling.

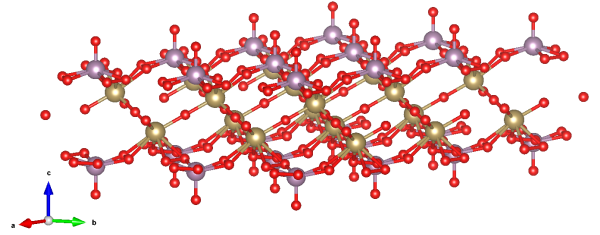FIG. SM44: DFT density of states. The insets shows the range around the Fermi level.

FIG. SM46: Bird-eye view of the crystal structure.

TABLE SM11: Structural parameters

	X[Å]	Y[Å]	Z[Å]
a1	3.0670	-5.3122	0.0000
a2	3.0670	5.3122	0.0000
a3	0.0000	0.0000	29.7696
Ta	1.5335	-0.8854	0.9405
Mo	1.5335	2.6561	2.8350
O	1.5335	2.6561	4.5001
O	3.3929	-1.1177	2.3804
O	0.8050	0.8411	2.3804
O	-0.3259	-1.1178	2.3804
O	2.2620	0.8411	2.3804
O	0.4025	-2.3795	2.3804
O	2.6645	-2.3795	2.3804
Ta	4.6005	0.8854	-0.9405
Mo	1.5335	2.6561	-2.8350
O	1.5335	2.6561	-4.5001
O	0.0000	0.0000	0.0000
O	1.5335	-2.6561	0.0000
O	3.0670	0.0000	0.0000
O	-0.4025	2.3795	-2.3804
O	2.7411	1.1178	-2.3804
O	2.2620	4.4711	-2.3804
O	0.3259	1.1178	-2.3804
O	3.4695	2.3795	-2.3804
O	0.8050	4.4711	-2.3804

* davide.grassano@epfl.ch

[1] K. Momma and F. Izumi, Journal of Applied Crystallography **44**, 1272 (2011).

[2] A. Marrazzo, M. Gibertini, D. Campi, N. Mounet, and N. Marzari, Nano Letters **19**, 8431 (2019).